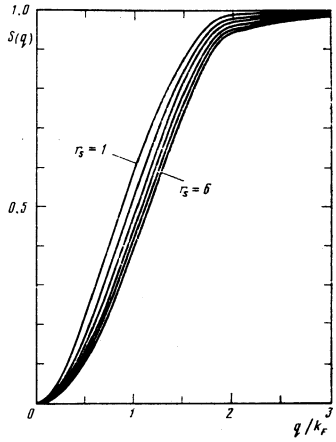

FIG. 2. Behavior of the static structure factor of an interacting electron gas in the metallic-density range.

solution of the system of Eqs. (23)–(25) at each iteration stage includes as a required element the recalculation of the static structure factor $S(\mathbf{q})$. This quantity is, as is well known, also of independent interest, since many physical characteristics of a system of interacting electrons are expressed by functionals of $S(\mathbf{q})$. We show therefore in Fig. 2 the results of the calculation of $S(\mathbf{q})$ for a number of values of the parameter r_s. In the limit of small q, the curves in Fig. 2 tend to an asymptotically correct relation (as $q \to 0$)

$$S(\mathbf{q}) \to q^2/2\alpha^2(3r_s)^{1/2},$$

while as $q \to \infty$ they are approximated by the formula

$$S(\mathbf{q}) \to 1 - 4\alpha r_s/3\pi q^4.$$

We note that in the approximation of Rajagopal and Jain the static structure factor has also the same asymptotic behavior (see Ref. 9 for the proof).

[1]D. Pines and P. Nozieres, The Theory of Quantum Liquids, Vol. 1, Benjamin, 1966.
[2]V. D. Gorobchenko and E. G. Maksimov, Usp. Fiz. Nauk **130**, 65 (1980) [Sov. Phys. Usp. **23**, 35 (1980)].
[3]V. D. Gorobchenko, Zh. Eksp. Teor. Fiz. **77**, 1197 (1979) [Sov. Phys. JETP **50**, 603 (1979)].
[4]D. N. Zubarev, Usp. Fiz. Nauk **71**, 71 (1960) [Sov. Phys. Usp. **3**, 320 (1960)].
[5]F. Toigoand T. O. Woodruff, Phys. Rev. **B2**, 3958 (1970).
[6]A. K. Rajagopal and K. P. Jain, Phys. Rev. **A5**, 1475 (1972).
[7]F. Brosens, L. F. Lemmens, and J. T. Devreese, Phys. Stat. Sol. (b) **74**, 45 (1976).
[8]D. N. Tripathy and S. S. Mandal, Phys. Rev. **B16**, 231 (977).
[9]A. Holas, P. K. Aravind, and K. S. Singwi, Phys. Rev. **B20**, 4912 (1979).
[10]F. Brosens, J. T. Devreese, and L. F. Lemmens, Phys. Stat. Sol. (b) **80**, 99 (1977).
[11]F. Brosens, J. T. Devreese, and L. F. Lemmens, J. Phys. F: Metal Phys, **10**, L27 (1980).
[12]K. S. Singwi, M. P. Tosi, R. H. Land, and A. Sjölander, Phys. Rev. **176**, 580 (1968).
[13]P. Vashistha and K. S. Singwi, Phys. Rev. **B6**, 875 (1972).
[14]J. T. Devreese, F. Brosens, and L. F. Lemmens, Phys. Rev. **B21**, 1349 (1980).
[15]F. Toigo and T. O. Woodruff, Phys. Rev. **B4**, 4312 (1971).

Translated by J. G. Adashko

Mode dependence of resonant absorption of ballistic phonons in CaF_2:Eu^{2+} crystals

A. V. Akimov and A. A. Kaplyanskiĭ

A.F. Ioffe Physicotechnical Institute, USSR Academy of Sciences

(Submitted 29 July 1980)
Zh. Eksp. Teor. Fiz. **80**, 767–774 (February 1981)

The anisotropy of absorption of longitudinal and transverse acoustic phonons in the 3×10^{11} band in a CaF_2:Eu^{2+} crystal is investigated experimentally and theoretically in the case of resonant interaction of the phonons with the electronic state $4f^65d(\Gamma_8^+)$ of the Eu^{2+} ion, split into a doublet by uniaxial compression of the crystal. The anisotropy agrees with the selection rules for transitions induced by dynamic deformation of a lattice in the field of a hypersound wave.

PACS numbers: 63.20.Mt

Experiments have been recently performed[1–3] on the behavior of nonequilibrium monochromatic terahertz acoustic phonons in uniaxially stressed CaF_2 and SrF_2 crystals activated with Eu^{2+} ions. The Eu^{2+} ions are situated in the lattices of these crystals in a cubic field of high symmetry O_h and some of the Eu^{2+} levels have orbital degeneracy. Use is made in Refs. 1–3 of the fact[4] that uniaxial deformation splits the orbitally degenerate radiative level Γ_8^+ of the excited $4f^65d$ configuration of Eu^{2+} into two, and the magnitude of the doublet splitting can vary smoothly in a range of several dozen reciprocal centimeters.[1,4] The existence of resonant single-phonon transitions between the components of the deformation doublet has made it possible to effect both fluorescent detection[1,2] of nonequilibrium monochromatic phonons with frequencies up to 2.4 THz [piezospectroscopic phonon detector (PPD)], as well as their generation in nonradiative relaxation of the optically excited ions.[1,3]

The ballistic character of the propagation of transverse phonons with $\nu \approx 0.5$ THz was demonstrated in

0038-5646/81/020387-05$02.40

Refs. 1 and 2 by the method of fluorescence detection of the phonons in CaF_2 and SrF_2 with Eu^{2+}. Ballistic phonon propagation makes it possible to study by the method of optical detection the resonant absorption of phonons belonging to separate modes.[5] This possibility was used by us here to investigate the mode dependence of resonant absorption of phonons in transitions between the levels of the deformation doublet Γ_8^+ of Eu^{2+} ions.

It was experimentally established that resonant absorption of transverse and longitudinal phonons with $\nu \approx 0.3$ THz is strongly anisotropic. It is shown that the spatial distribution of the absorption corresponds to selection rules of the "quadrupole" type for transitions induced by dynamic deformation of the lattice by acoustic phonons. Quantitative estimates are presented of the cross section for phonon absorption and for the probability of phonon emission in transitions between the levels of the deformation odulet. It is noted that the role of dynamic rotations in single-phonon transitions in a PPD is negligible.

EXPERIMENTAL RESULTS

We used in the experiments single-crystal $CaF_2 + 0.01\% Eu^{2+}$ samples (Fig. 1a) in the form of right $6 \times 4 \times 1.5$ mm parallelepipeds. Three edges of the samples were parallel to the crystallographic axes $[100]_x$, $[010]_y$, and $[001]_z$ or to $[001]_z$, $[110]_{xy}$, and $[1\bar{1}0]_{xy}$. The sample temperature was 2 K. The lateral (small) surface of the sample was coated with a 1×1 mm constantan film. When the film was heated by $\Delta t = 200$ nsec current pulses at a repetition frequency 10 kHz, thermal phonon pulses were injected in the crystal.

The crystal was illuminated by a DRSh-250 mercury lamp with a UFS-5 filter (365 nm Hg line). Part of the Eu^{2+} ions were excited into the $4f^6 5d$ (Γ_8^+) state, and the transitions from Γ_8^+ into the ground state $^8S_{7/2}$ ($4f^7$) give a zero-phonon 4130 Å luminescence line. The samples were subjected to a uniaxial compression along the vertical axis P, and the Γ_8^+ level was split thereby into a deformation doublet W_1, W_2. At a temperature 2 K the lowest (W_1) sublevel of the Γ_8^+ deformation doublet is predominantly populated, since the splitting $\Delta = W_2 - W_1 \ll kT$. A strong stationary luminescence is then observed, corresponding to the zero-phonon transition $W_1(\Gamma_8^+) \rightarrow {}^8S_{7/2}$. The luminescence light is gathered through a light pipe from a small volume d inside the sample, located at a distance $x = 2$–4 mm from the heater h. When the thermal pulses enter the volume d, phonons of frequency $h\nu = \Delta$ induce single-phonon transitions $W_1 \rightarrow W_2$, and this produces in the luminescence transitions from the upper level W_2 (Γ_8^+). In the experiments we measured the fluorescence pulses $I_{W_2}(t)$ in the zero-phonon line W_2 (Γ_8^+) $\rightarrow {}^8S_{7/2}$ (see Fig. 1b).

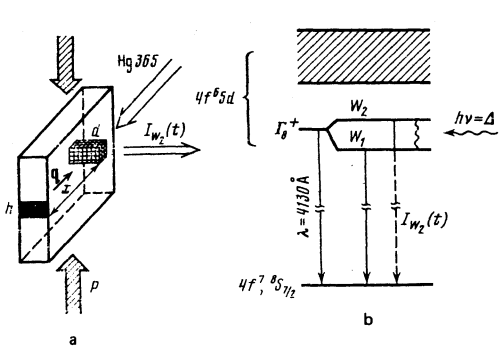

FIG. 1. Experimental setup.

In accord with Refs. 1 and 2, in deformation splittings $\Delta \approx 0.3$ THz (~10 cm^{-1}) the fluorescence pulses have steep leading fronts, attesting to a ballistic flight of phonons of corresponding frequency from the heater h to the detector d. The "ballistic" front precedes the more gently sloping pulse rise corresponding to a gradual arrival of the phonons at the detector not along straight trajectories (owing to scattering in the volume and by the surfaces of the sample). The strong nonresonant scattering of the phonons by the CaF_2 structure defects manifests itself in an overall stretching of the pulse $I_{W_2}(t)$ induced mainly by "isotropized" phonons from different modes. Only in the region of the ballistic front of $I_{W_2}(t)$ does an interaction appear with an individual molecule, determined by the h–d propagation direction and by the polarization (arrival time) of the phonon.

We have observed that the picture of the $I_{W_2}(t)$ ballistic fronts depends strongly on the direction of the compression axis P in the crystal, on the direction $\mathbf{q}$ of the phonon propagation (the h–d line), and on the phonon polarization. Depending on these conditions, both ballistic transverse (TA) and ballistic longitudinal (LA) phonons appear in the $I_{W_2}(t)$ fluorescence pulses and reach the detector.

Figure 2a shows the $I_{W_2}(t)$ pulse obtained in a sample

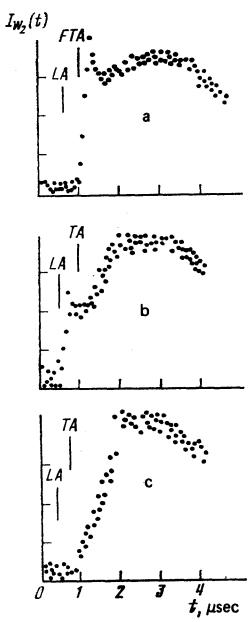

FIG. 2. Fluorescence pulses I_{W2} (T). a) $P \parallel [001]_z$, $\mathbf{q} \parallel [110]_{xy}$, $\Delta = 8$ cm^{-1}, $x = 4$mm; b) $P \parallel [001]_z$, $\mathbf{q} \parallel [010]_{xy}$, $\Delta = 9$ cm^{-1}, $x = 3.5$ mm; c) $P \parallel [110]_{xy}$, $\mathbf{q} \parallel [001]_z$, $\Delta = 9$ cm^{-1}, $x = 2.5$ mm.

compressed along $P\|[001]_z$ at a direction $\mathbf{q}\|[110]_{xy}$. One ballistic front is observed, with a position corresponding to the propagation velocity of the transverse sound (in Fig. 2, the calculated times of arrival of the TA and LA phonons are indicated by vertical bars.[1)] Figure 2b shows the pulse $I_{W_2}(t)$ in a sample compressed along $P\|[001]_z$, but with the phonons propagating along $\mathbf{q}\|[010]_y$. In this case a front is observed at an arrival time corresponding to the longitudinal LA phonons. Figure 2c shows the $I_{W_2}(t)$ pulse for a sample compressed along $P\|[110]_{xy}$ at a direction $\mathbf{q}\|[001]_z$. It is seen that in this case the pulse $I_{W_2}(t)$ has no steep leading front at all.

INTERPRETATION OF THE RESULTS

The amplitude of the ballistic fluorescence pulse

$$I_{W_2}(t)\sim n_\Delta(t)\sigma N^*, \tag{1}$$

where $n_\Delta(t)$ is the number of phonons of frequency Δ in the detector, σ is the cross section for resonant absorption of a phonon by the excited Eu^{2+} ion in $W_1 \to W_2$ transitions, and N^* is the concentration of the excited ions. The experimentally observed dependence of the picture of the ballistic $I_{W_2}(t)$ pulses on the phonon propagation direction and polarization is attributed by us mainly to the strong mode dependence of the cross section σ for one-phonon absorption.

The properties of one-phonon transitions between the sublevels W_1 and W_2 are closely connected with the peculiarities of the behavior of the state $4f5d$ (Γ_8^+) of the Eu^{2+} ions under static deformation of the crystal.[4] The level Γ_8^+ behaves under static deformation like the orbitally doubly degenerate level Γ_3^+ ($\Gamma_8^+=\Gamma_3^+\times D^{1/2}$, where $D^{(1/2)}$ is the representation for the spin $\pm\frac{1}{2}$).[4] The basis functions of Γ_3^+ can be chosen[4,7] in the form $\varphi_1=2z^2-x^2-y^2$ and $\varphi_2=3^{1/3}(x^2-y^2)$. The operator of the perturbation by the strain is

$$H'=\Sigma V_{ik}\varepsilon_{ik}, \tag{2}$$

where ε_{ik} are the components of the strain tensor and V_{ik} are electron operators with the transformation properties of a second-rank tensor. The perturbation matrix on the functions φ_1 and φ_2 is of the form[7]

$$\begin{vmatrix} a\Sigma\varepsilon_{ii}-b(2\varepsilon_{zz}-\varepsilon_{xx}-\varepsilon_{yy}), & \sqrt{3}\,b(\varepsilon_{xx}-\varepsilon_{yy}) \\ \sqrt{3}\,b(\varepsilon_{xx}-\varepsilon_{yy}), & a\Sigma\varepsilon_{ii}+b(2\varepsilon_{zz}-\varepsilon_{xx}-\varepsilon_{yy}) \end{vmatrix}, \tag{3}$$

where a and b are the deformation potentials of the level.[2)] For the compression of interest to us along $P\|[001]_z$ and $P\|[110]_{xy}$ the off-diagonal elements of (3) are equal to zero ($\varepsilon_{xx}=\varepsilon_{yy}$). In both these cases the sublevels W_1 and W_2 of the split state Γ_8^+ correspond to the functions φ_1-W_1 and φ_2-W_2 at $P\|[001]_z$ and φ_1-W_2 and φ_2-W_1 at $P\|[110]_{xy}$.[4,7] The level splitting $\Delta=W_2-W_1$ is

$$\Delta=\frac{4b}{C_{11}-C_{12}}p \quad \text{at} \quad P\|[001]_z,$$
$$\Delta=\frac{2b}{C_{11}-C_{12}}p \quad \text{at} \quad P\|[110]_{xy},$$

where C_{11} and C_{12} are the elastic constants and p is the uniaxial compression stress. From the data of Ref. 4 on the splitting of the Γ_8^+ level of $CaF_2:Eu^{2+}$ it follows that the deformation potential is $b=3.3\times10^3$ cm^{-1}.

Single-phonon transitions between the electronic levels $W_1 \rightleftarrows W_2$ of the Eu^{2+} ion are induced by modulation of the crystal field at the resonant frequency $\nu=(W_2-W_1)/h$, which is induced by the passage of the phonon. Since the Eu^{2+} ion is located in an O_h centrosymmetric crystal field and the levels W_1 and W_2 have like parity, the active perturbation should be even. For long-wave acoustic phonons such a perturbation is the dynamic lattice deformation in the field of the sound wave

$$\mathbf{u}(\mathbf{r},t)=\mathbf{u}e^{i(\omega t-\mathbf{qr})}, \tag{4}$$

where $\mathbf{u}$ is the polarization (displacement) vector, $\mathbf{q}$ is the wave vector, and $\omega=2\pi\nu$ is the frequency of the acoustic phonon. The strain produced by the wave (4) is given by

$$\varepsilon_{ik}=(u_iq_k+u_kq_i)/2, \quad i,k=x,y,z. \tag{5}$$

The operator of the perturbation due to the dynamic strain is of the form (2).

To calculate the cross section for the absorption of acoustic phonons by Eu^{2+} ions it is convenient to use the expression[8]

$$\sigma(\nu)=\frac{2\pi^2\nu}{h\rho v^3}\frac{|\langle1|H'|2\rangle|^2}{|u|^2|q|^2}g(\nu), \tag{6}$$

where ρ is the density, v is the phase velocity of the sound, $g(\nu)$ describes the line contour [$\int g(\nu)d\nu=1$], and $\langle1|H'|2\rangle$ is the matrix element of the perturbation (2) between the functions φ_1 and φ_2. It follows from (3) and (5) that

$$|\langle1|H'|2\rangle|^2=3b^2|u|^2|q|^2(n_xm_x-n_ym_y)^2, \tag{7}$$

where n_i and m_i are the direction cosines of the vectors $\mathbf{u}$ and $\mathbf{q}$. Substitution of (7) in (6) yields

$$\sigma(\nu)=\frac{6\pi^2b^2\nu g(\nu)}{h\rho v^3}(n_xm_x-n_ym_y)^2. \tag{8}$$

It follows from (8) that the $W_1 \to W_2$ absorption cross section is anisotropic and depends both on the propagation direction $\mathbf{q}$ and on the polarization $\mathbf{u}$ of the acoustic phonon. The anisotropic distribution (8) is "tied" to the crystallographic axes x, y, and z by definite compression directions ($[001]_z$ or $[110]_{xy}$). Figure 3 shows the absorption angular dependence calculated from (8) for phonons propagating in the cube planes $(001)_z$ (xy plane) and $(010)_y$ (zx plane). The calculation was made for longitudinal (LA), fast transverse (FTA), and slow transverse (STA) phonons. Account was taken of the elastic anisotropy of CaF_2, which leads to a deviation of $\mathbf{u}$ from $\mathbf{u}\|\mathbf{q}$ (quasilongitudinal phonons) and from $\mathbf{u}\perp\mathbf{q}$ (quasitransverse phonons). The directions $\mathbf{u}$ for LA and TA waves with given $\mathbf{q}$ were determined by the usual procedure of solving the equations of acoustics.[9] We used the low-temperature acoustic constants of CaF_2 (Ref. 6): $C_{11}=17.4\times10^6$ N/cm^2, $C_{12}=5.6\times10^6$ N/cm^2, and $C_{44}=3.6\times10^6$ N/cm^2. It is seen from Fig. 3 that the angular dependence of σ in the (001) plane has a complicated character and is different for LA and TA phonons, with $\sigma\equiv0$ for individual modes in several high-symmetry directions.

The calculation results agree well with the experimental data. Thus, at $P\|[001]_z$ and $\mathbf{q}\|[010]_y$ the $W_1 \to W_2$ transitions are theoretically allowed only for LA

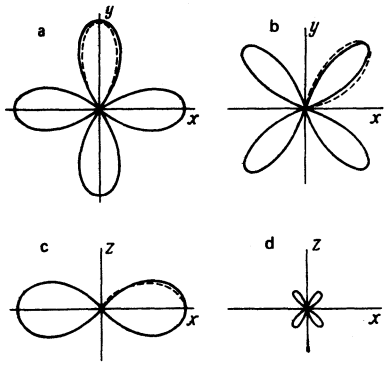

FIG. 3. Polar diagram of the absorption cross section σ as a function of the change of the direction of q: a, b) in the xy plane; c, d) in the zx plane; a, c) for *LA* phonons, b, d) for *LTA* phonons, $\sigma \equiv 0$ for *STA* phonons. The diagram of σ for the case of another isotropy is shown dashed.

phonons. At $\mathbf{q} \| [110]_{xy}$, on the contrary, transitions are allowed only for FTA phonons. At $P \| [001]_z$, in full agreement with this conclusion, ballistic fronts $I_{W_2}(t)$ are induced only by LA phonons at $\mathbf{q} \| [010]_y$ and only by TA phonons at $\mathbf{q} \| [110]_{xy}$ (see Figs. 2a and 2b). At $P \| [110]_{xy}$, for phonons with $\mathbf{q} \| [001]_z$, transitions for LA and TA phonons are theoretically forbidden. In experiment, in fact, no ballistic fronts $I_{W_2}(t)$ are observed for LA and TA phonons in this direction of q (Fig. 2c).

It follows from (8) that the absorption cross section is proportional to v^{-3}, and consequently the absorption of LA phonons (velocity $v \approx 7$ km/sec) should be 5–6 times less than the absorption of TA phonons ($v \approx 4$ km/sec). In experiment, however, the amplitudes of the ballistic pulses from LA and TA phonons are comparable for the allowed directions. To explain this fact account must be taken of the possible role played by the phonon focusing due to the elastic anisotropy of the CaF_2.[10] According to the calculations[10] the FTA phonons are focused in CaF_2 along the [110] diagonals, and the LA phonons are focused in the directions of the cube axes [001]; the degree of focusing (the coefficient of amplification of the phonon flux) for the LA phonons (=3.21) is larger than for the FTA phonons (=1.72). Thus, the larger number n_Δ of LA phonons in the $[010]_y$ direction can compensate in part for the smallness of the cross section σ for the absorption of these phonons [see (1)]. At the same time, the difference between the $I_{W_2}(t)$ pictures (Figs. 2b and 2c) for the two directions P of phonon propagation along the cube axis shows that the focusing is not responsible for the basic character of the anisotropy of the $I_{W_2}(t)$ pulses.

The deformation potential $b = 3.3 \times 10^3$ cm^{-1} of the Γ_8^+ level, known from piezospectroscopic experiments,[4] can be used to estimate the absolute values of the cross section (8). It follows from (8) that at the center of the phonon line the cross section (at a unity angle factor) is

$$\bar{\sigma} = 6\pi^2 b^2 \nu / h\rho \bar{v}^3 \Delta\nu, \tag{9}$$

where $\Delta\nu$ is the width of the $W_1 - W_2$ phonon line. Assuming $\Delta\nu = 1$ cm$^{-1} \approx 3 \times 10^{10}$ sec^{-1} (inhomogeneous broadening estimated from the width of the 4130 Å zero-phonon line $\Gamma_8^+ - {}^8S_{7/2}$), $\nu = 3 \times 10^{11}$ sec^{-1} (for $\Delta = 10$ cm^{-1}), ρ13.2 g/cm^3, $\bar{v}_L = 7$ km/sec, and $\bar{v}_T = 4$ km/sec, we obtain for the absorption of the longitudinal and transverse phonons the values $\bar{\sigma}_L \approx 3.6 \times 10^{-14}$ and $\sigma_T \approx 2 \times 10^{-13}$ cm^2.

We determine now the lifetime of the upper deformation sublevel W_2 relative to a transition with emission of a phonon $h\nu = W_2 - W_1$. According to the detailed-balancing principle, this time is connected with the total cross section for the absorption of three phonon modes, obtained by integrating (8) over the angles:

$$T_1^{-1} = \frac{6\pi^2 b^2 \nu^3}{h\rho} \left[\frac{\bar{\Omega}_1}{\bar{v}_L^5} + \frac{\bar{\Omega}_2 + \bar{\Omega}_3}{\bar{v}_T^5} \right], \tag{10}$$

where

$$\bar{\Omega}_i = \int_0^{4\pi} [m_x^{(i)} n_x - m_y^{(i)} n_y] d\Omega$$

are integrals over the total solid angle ($i = 1, 2, 3$) and are equal to $\bar{\Omega}_1 = (16/15)\pi$, $\bar{\Omega}_2 = (4/15)\pi$, and $\bar{\Omega}_3 = (4/3)\pi$. The derivation of (10) and the calculation of $\bar{\Omega}_i$ were performed in the elastic-isotropy approximation ("pure" LA and TA modes, absence of focusing). Substituting in (10) the parameters indicated above, we get $T_1^{-1} = 2 \times 10^{10}$ sec^{-1} at $\nu = 10$ cm^{-1}.

It is seen from (10) that the probability of the one-phonon decay $T_1^{-1} \sim \nu^3$, and is consequently proportional to the cube of the uniaxial compression. Important characteristics of the piezospectroscopic phonon detector (PPD) such as the absorption cross section (σ) and the "time constant" (T_1^{-1}) turn out therefore to depend on the level splitting. In the PPD the static deformation splitting and the probabilities of the single-phonon transitions are described by one and the same parameter ($\Delta \sim |b|$; $\sigma, T_1^{-1} \sim |b|^2$). Since for the operation of PPD in the terahertz band it is important to have activated crystals with large deformation potentials (b), the probabilities of single-phonon transitions are always large.[3)]

At the frequency $\nu = 1$ cm^{-1} the calculated value $T_1^{-1} \approx 2 \times 10^7$ sec^{-1} is comparable with the reciprocal radiative lifetime of the Γ_8^+ level in $CaF_2:Eu^{2+}$ crystals.[12] One can thus expect in the splittings of Γ_8^+ ($\Delta \approx 1$ cm^{-1}) deviations from a Boltzmann equilibrium between the sublevels. Notice should be taken in this connection of the experimental observation of deviation of the Γ_8^+ sublevels from a Boltzmann distribution in a magnetic field.[12,13]

The case $CaF_2:Eu^{2+}$ investigated here shows that an impurity ion in a crystal is an anisotropic resonant phonon scatterer. Equation (8) gives one of the examples of the spatial distribution of the acoustic phonon absorption (emission).[4)] The actual form of (8) follows in essence directly from the form of the strain matrix element between combining levels, which in this case is $\sim \varepsilon_{xx} - \varepsilon_{yy}$. It is possible to calculate in exactly the same manner the spatial distributions for single-phonon transitions between other arbitrary strain sublevels of local centers in uniaxially stressed crystals. For centers with cubic symmetry in cubic crystals it is possible to use directly in such a calculation the strain matrix elements in the form given in Ref. 7

(with σ_{ik}).

The perturbation that induces the single-phonon transitions was taken in the present paper to be only the dynamic strains ε_{ik}. They are expressed in terms of products of components of u and q [Eq. (5)] that transform like a second-rank symmetric tensor. Yet an active role can be played in principle in the transitions also by dynamic rotations $\omega = \frac{1}{2}\mathbf{u} \times \mathbf{q}$ (Refs. 8 and 15), which have the transformation properties of an axial vector. The relative contribution of the strains and of the rotations to the matrix element $\langle 1|H'|2\rangle$ of a single-phonon transition is determined by the ratio of the deformation potential (b) to the transition energy (Δ). In our case $b \approx 3 \times 10^3$ cm^{-1} and $\Delta_{max} \approx 30$ cm^{-1}, therefore the contribution of the rotations to the transition probability is $\sim(\Delta/b)^2 \approx 10^{-4}$ and can be neglected. In general, the role of the rotations, compared with strain, can be regarded as small for all PPD of the terahertz band, for which $b \gg \Delta$ always.

The authors thank G. E. Pikus and E. L. Ivchenko for a helpful discussion.

[1)]The velocities of the TA and LA phonons were calculated from the elastic constants of CaF_2 at $T = 4$K.[6] The velocity indicated for the phonon propagation direction $\mathbf{q} \parallel [110]$ is that of the fast FTA phonons.

[2)]A perfectly analogous matrix for Γ_3^+ with the corresponding parameters A and B is given in Ref. 7 [Eq. (6)] for the stresses δ_{ik}. The relations between the parameters (3) and (6) of Ref. 7 are $b = (C_{11} - C_{12})B$ and $a = (C_{11} + 2C_{12})A$.

[3)]The calculated transition probability in CaF_2:Eu^{2+} crystals at $\nu = 30$ cm^{-1} and $T_1^{-1} \approx 6 \times 10^9$ sec^{-1} exceeds by two orders of magnitude, say, the probability of the $2\bar{A} \to \bar{E}$ transition in Cr^{3+} ions in ruby ($\nu = 29$ cm^{-1}, $T_1^{-1} = 3 \times 10^9$ sec^{-1}, Ref. 11).

[4)]We point out a general analogy between the spatial distribution of acoustic-phonon emission (absorption) and the distribution of electromagnetic radiation in the case of electric quadrupole transtions. The latter are known[14] to be described by an expression of the type $|\Sigma_{ik} e_i q_k Q_{ik}|^2$, where e is the electric vector, q is the wave vector of the electromagnetic wave, and $Q_{ik} = ex_i x_k$ is the electric quadrupole moment of the transition.

[1]W. Eisfeld and K. F. Renk, Appl. Phys. Lett. **34**, 481 (1979).
[2]A. P. Abramov, I. N. Abramova, I. Ya Gerlovin, and I. K. Razumova, Fiz. Tverd. Tela (Leningrad) 22, 946 (1980) [Sov. Phys. Solid State 22, 556 (1980)].
[3]A. V. Akimov, A. A. Kaplyanskiĭ, and A. L. Syrkin, Pis'ma Zh. Eksp. Teor. Fiz. **32**, 136 (1980) [JETP Lett. **32**, 124 (1980)].
[4]A. A. Kaplyanskiĭ and A. K. Przhevuskiĭ, Opt. Spektrosk. **19**, 597 (1965) [Opt. Spectrosc. **19**, 331 (1965)].
[5]A. A. Kaplyanskiĭ, S. A. Basun, V. A. Rachin, and R. A. Titov, Pis'ma Zh. Eksp. Teor. Fiz. **21**, 438 (1975) [JETP Lett. **21**, 200 (1975)].
[6]W. Hayes, Crystals with the Fluorite Structure, Oxford, 1947, p. 47.
[7]A. A. Kaplyanskiĭ, Opt. Spektrosk. **16**, 1031 (1964) [Opt. Spectrosc. **16**, 557 (1964)].
[8]H. Kinder, Z. Physik **B262**, 295 (1973).
[9]J. W. Tucker and V. W. Rampton, Microwave Ultrasonics in Solid State Physics, North Holland, 1972.
[10]H. Maris, J. Acoust. Soc. Am. **50**, 812 (1971).
[11]M. Blume, R. Orbach, A. Kiel, and S. Geschwind, Phys. Rev. **139**, A314 (1965).
[12]P. Kisliuk, H. H. Tippins, and C. A. Moore, Phys. Rev. **171**, 336 (1968).
[13]M. V. Eremin, B. P. Zakharchenya, A. Ya. Ryskin, and Yu. Stepanov, Opt. Spektrosk. **33**, 1128 (1971) [*sic*]. M. A. Él'yashevich, Spektry redkikh zemel' (Rare Earth Spectra), GITTL, 1953, part I, §9.
[15]R. L. Melcher, Phys. Rev. Lett. **28**, 1465 (1972).

Translated by J. G. Adashko

Anomalous skin effect on a rough surface in a magnetic field

L. A. Fal'kovskiĭ

L. D. Landau Institute of Theoretical Physics, USSR Academy of Sciences
(Submitted 4 August 1980)
Zh. Eksp. Teor. Fiz. **80**, 775–786 (February 1981)

The impedance of a metal in a magnetic field parallel to the surface is calculated with allowance for the scattering of the conduction electrons by surface roughnesses. The monotonic part of the impedance is determined by the multiply reflected electrons and depends on the competition of their scattering by bulk or surface defects. The cyclotron oscillations are small, except when the mean free path is very large and in a narrow vicinity of the resonance the contribution of the electrons that do not collide with the surface becomes predominant.

PACS numbers: 73.25. + i

1. INTRODUCTION

The surface impedance of a metal in a magnetic field parallel to the surface depends substantially on the character of the scattering of the conductions electrons from the sample boundary. The reason is that the influence of the surface comes into play at a distance determined either by the electron mean free path l or by the Larmor radius r, i.e., by parameters that can be large compared with the skin-layer depth δ (we assume

 0038-5646/81/020391-07$02.40